Chemistry and Physics of Lipids 200 (2016) 11–23

Contents lists available at ScienceDirect

Chemistry and Physics of Lipids

journal homepage: www.elsevier.com/locate/chemphyslip

Lyotropic behavior of Gelucire 50/13 by XRD, Raman and IR spectroscopies according to hydration

M. El Hadri[a], A. Achahbar[a], J. El Khamkhami[a], B. Khelifa[b,e], V. Faivre[c], O. Abbas[d], S. Bresson[e,*]

[a] Laboratoire de Physique de la Matière Condensée, Université Abdelmalek Essaâdi, Tétouan, Morocco
[b] Faculté des sciences, Université d'Artois, Lens, France
[c] Equipe Physico-chimie des Systèmes Polyphasés, UMR CNRS 8612, Labex LERMIT Université Paris Sud, France
[d] Walloon Agricultural Research Centre (CRA-W), Valorisation of Agricultural Products, Department, Food and Feed Quality Unit (U15), 'Henseval Building', Chaussée de Namur 24, 5030 Gembloux, Belgium
[e] Laboratoire de Physique des Systèmes Complexes, Université Picardie Jules Verne, 33 rue St. Leu, 80039 Amiens cedex, France

ARTICLE INFO

Article history:
Received 12 February 2016
Received in revised form 5 May 2016
Accepted 10 May 2016
Available online 16 June 2016

Keywords:
Gelucire 50/13
Triglycerides
PEG
Hydration
ATR FTIR
Spectroscopy Raman

ABSTRACT

The present paper discuss the structural and vibrational properties of polyoxyethylene glycol glycerides (Gelucire 50/13) during the hydration with increasing water from 0% to 80%. The Gelucire 50/13 used as sustained release matrix forming agent in pharmaceutical applications and it was essentially studied by Small and Wide Angle X-ray Scattering (SWAXS), Fourier transform infrared spectroscopy (FTIR) and Raman spectroscopy according to the rate of hydration. The hydration behavior of this amphiphilic excipient has been investigated in the spectral range 4000–0 cm^{-1} in Raman spectroscopy, and 4000–600 cm^{-1} in FTIR. At increasing water contents Gelucire 50/13 forms successive bicontinuous to micellar supramolecular structures, and the vibrational changes were directly correlated with this conformational changes of the Gelucire structure. Overall, Raman and IR spectroscopy clearly demonstrated that the different functional groups studied could be characterized independently, allowing for the understanding of their role in Gelucire polymorphism.

1. Introduction

Gelucires are a group of amphiphilic excipients which have been widely studied as controlled release matrices (Mouricout et al., 1990). The incorporation of drugs into Gelucires has been reported to increase the dissolution rate of poorly soluble drugs, often leading to improved drug bioavailability (Damian et al., 2000; Gines et al., 1995; Gupta et al., 2001; Perissutti et al., 2000). One compound from this group is Gelucire 50/13. This amphiphilic excipient, which has a mean Hydrophilic-Lipophilic Balance of 13 and a melting temperature around 50 °C, consists of a mix of mono-, di-, triacyl glycerol (around 20% in weight) and monoacyl polyoxyethylene glycols and diacyl poly-oxyethylene glycols labeled, respectively, MPEG and DPEG. It has a wide variety of applications in pharmaceutical formulations as the preparation of fast release and sustained release formulations.

In pharmaceutical applications, it is important to know how the excipients interact with the drug, and how the mixture behaves during manufacturing, storage as well as during administration. These behaviours depend on the effects of temperature and hydration on the physical state of the excipient. Moreover, after administration, the mixture will be immersed in body fluids, and it is important to know what are the pathways for dissolution in this aqueous medium. Thus, water flux has crucial role on drug release from lipid based matrices (Pivette et al., 2012) and it would be very sensitive to the presence of amphiphilic excipients as Gelucire 50/13. There have been a few studies of the thermal behaviour of dry Gelucires (Craig and Newton, 1991; Sutananta et al., 1994), but, to our knowledge, few systematic study of their hydration behavior (Svensson et al., 2004). The aim of this project was to investigate the behaviour of the Gelucire 50/13 when exposed to water, at ambient temperature. During hydration, we have investigated the state of Gelucire 50/13 mixed with known amounts of water (from 0% to 80%) by Raman and FTIR spectroscopy. The nature of the phases that are formed and their structural parameters were also studied by XRD. The study of Gelucire by Raman and FTIR spectroscopy brings a lot of information about the intra and

* Corresponding author.
E-mail address: sergebresson@yahoo.fr (S. Bresson).

http://dx.doi.org/10.1016/j.chemphyslip.2016.05.005
0009-3084/

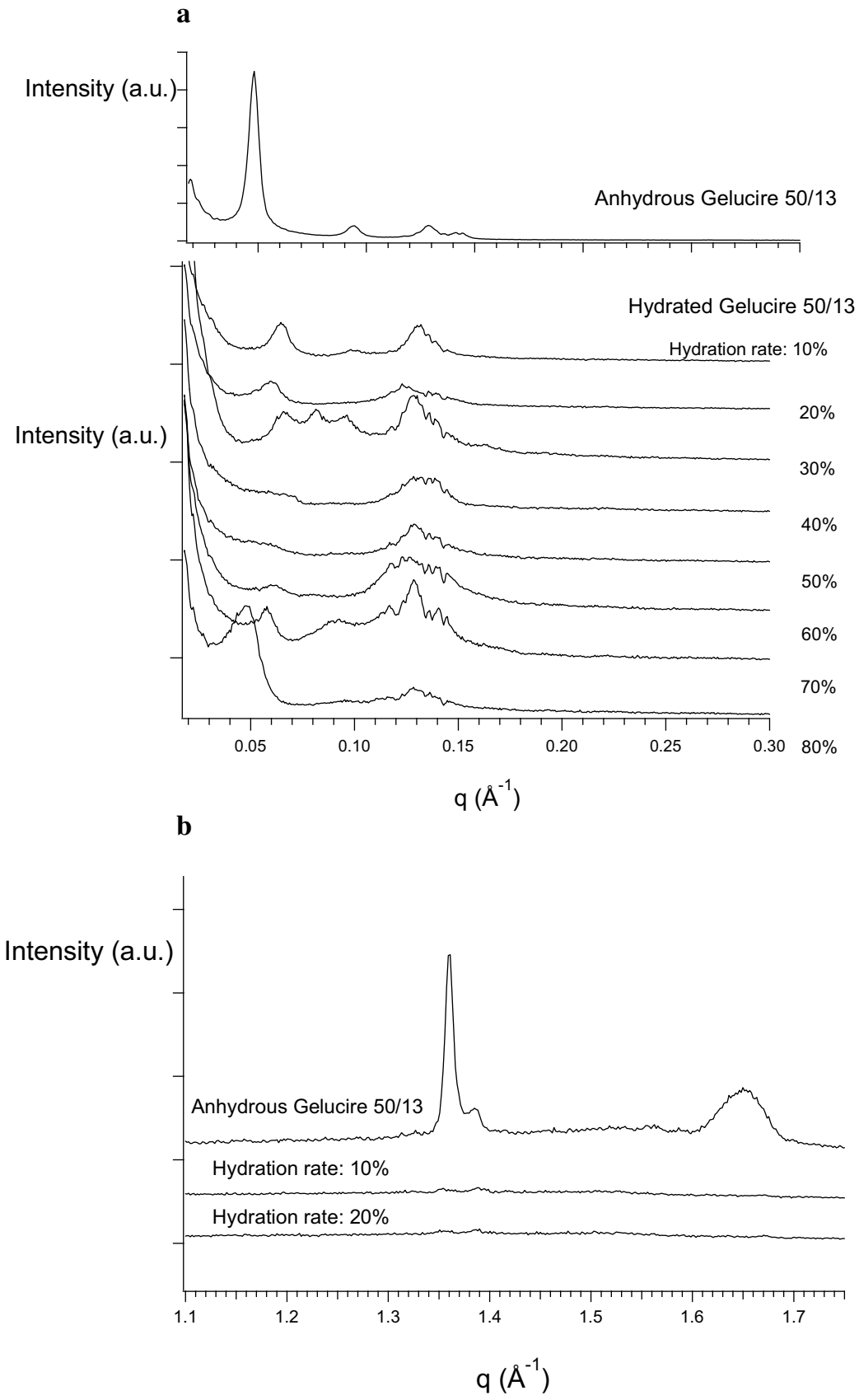

Fig. 1. SAXS (a) and WAXS (b) diffractogram of Gelucire 50/13 as a function of the rate of hydration.

intermolecular interactions and would facilitate the understanding of these with the aim of improving the formulation of active products and then their efficiency in the body. Raman and FTIR spectroscopy's are a vibrational spectroscopy's techniques that can provide a sensitive, relatively quick, non-destructive means of probing molecular structure in solid and liquid lipids (Hu et al., 2005; Schoukens and De Clerck, 2005; Bresson et al., 2006; Da Silva et al., 2009). The most sensitive Raman-IR-active features include the O—H, C—H and C—C stretching vibrations, notably the ν(O—H) stretching region (3600–3200 cm^{-1}), the ν(C—H) stretching region (3000–2800 cm^{-1}), the ν(C—C) skeletal modes (1200–1000 cm^{-1}), the $\delta(CH_2)$ deformation region (1500–1400 cm^{-1}) and the $\tau(CH_2)$ twisting region (1300–1250 cm^{-1}). These regions provide insight into the degree of alkyl chain coupling, intramolecular motion, the relative populations of *gauche* (distorted) and *trans* conformers as well as chain twisting and bending. In the present article we want study the effect of the hydration in all these regions by IF-Raman and FTIR, and to compare these results with the results in DRX.

2. Materials and methods

2.1. Preparation of the Gelucire 50/13

Small pellets of Gelucire 50/13 were supplied by Gattefossé S. A. S., St Priest (France). Gelucire 50/13 is synthesized by an alcoholysis/esterification reaction using as starting materials hydrogenated palm oil and PEG 1500, equivalent to approximately 34 monomer units —CH_2—CH_2—O—, and ended by two alcohol groups.

2.2. Preparation of the hydrated Gelucire 50/13

Chloroformic solutions of Gelucire 50/13 were prepared to homogenize the composition and were evaporated under a gentle stream of nitrogen to obtain lipid films. Residual organic solvent was eliminated under vacuum (< 1 mPa). The films were hydrated with adequate amount of water and mixed with vortex and ultrasonic water bath. Samples were prepared at least 24 h before analysis in order to reach hydration equilibrium.

2.3. FT-Raman and FT-IR spectroscopy

The measurements were carried out at the Walloon Agricultural Research Center (Cra-w), Belgium.

All attenuated total reflectance Fourier transform mid-infrared (ATR/FTIR) spectra were acquired using a Vertex 70-RAM II Bruker spectrometer (Bruker Analytical, Madison, WI) operating with a Golden Gate TM diamond ATR accessory (Specac Ltd, Slough, UK). FTIR/ATR spectra [4000–600 cm^{-1}] were collected with a resolution of 1 cm^{-1} by co-adding 64 scans for each spectrum at room temperature.

FT-RAMAN spectra were acquired using a Vertex 70-RAM II Bruker FT-RAMAN spectrometer. This instrument is equipped with an Nd: YAG laser (yttrium aluminium garnet crystal doped with triply ionised neodymium) with an incident laser wavelength at 1064 nm (9398.5 cm^{-1}). The RAM II spectrometer is equipped with a liquid-nitrogen cooled Ge detector. FT-RAMAN spectra [4000–45 cm^{-1}] were collected with a resolution of 1 cm^{-1} by co-adding 128 scans for each spectrum at room temperature.

2.4. X-ray diffraction (XRD)

X-ray scattering experiments were performed on the 5.2 L beamline at ELETTRA Synchrotron Light Laboratory (Trieste, Italy). The energy and wavelength of the incident X-ray beam were 8 KeV and 1.54 Å respectively. The samples were thermostated in the laboratory made sample holder, Microcalix, allowing both sample temperature control and simultaneous differential scanning calorimetry analysis. Small-angle (SAXS) and wide-angle (WAXS) X-ray scattering patterns were recorded simultaneously using a 2D single photon counting detector (Pilatus 100K) based on hybrid pixel technology (Dectris, Swiss) and a position-sensitive linear gas detectors filled with an argon-ethane mixture respectively. After 2D-image treatment in the SAXS experiments, the scattered intensity was reported as a function of the scattering vector $q = 4\pi \sin\theta/\lambda = 2\pi/d$, where 2θ is the scattering angle, λ is the wavelength and d is the repeat distance between two reticular plans. The calibration of the WAXS and SAXS detectors were achieved using pure tristearine (2Lβ form), characterized by short spacings of 4.59, 3.85 and 3.70 Å ± 0.01 Å and silver behenate characterized by a long spacing of 58.380 Å ± 0.001 Å respectively. The samples were loaded into quartz capillaries (Quarzkapillaren, Germany) with external diameter of 1.4 ± 0.1 mm and a wall thickness of 0.01 mm. All data were analyzed with the IGOR Pro software (WaveMetrics, Inc., USA).

3. Results and discussion

Small- and wide angles X-ray diffraction was used to investigate the lyotropic behaviour of Gelucire 50/13. Fig. 1a shows the SAXS diffractograms obtained with anhydrous and hydrated Gelucire 50/13. Hydration rates from 10% to 80% have been studied. In the WAXS region, a focus on anhydrous and 10%-hydrated mixture is given on Fig. 1b as higher hydration rates are poor in structural information. All the diffraction data are summarized in Table 1.

Previous papers provide substantial descriptions of the anhydrous Gelucire 50/13 (Jannin et al., 2014; Rosiaux et al., 2014; Qi

Table 1
Position of the diffraction peaks extracted from the SWAXS diffractograms. Values in italic have been attributed to the glyceride-rich phase of the Gelucire 50/13 while the others are descriptors of the PEG-esters fraction. Concerning the q-WAXS value around 1.52, the intensity of the corresponding peak is very weak and its detection by the Igor macro was not systematic.

Hyd. rate	q-SAXS (Å^{-1})	q-WAXS (Å^{-1})
0	0.04823; 0.09407; *0.12844*; 0.14352; *0.25814; 0.38785*	1.361; 1.653
10	0.03208; 0.06452; 0.09800; *0.13087*	1.369(vw); *1.518* (vw); 1.659(vw)
20	0.05970; *0.12422*; 0.13870; *0.39800*	*1.518*(vw)
30	0.06573; 0.08141; 0.09588; *0.12844*; 0.16282; 0.19174	*1.525*(vw)
40	0.07056; *0.12844*	
50	0.05970; *0.12844*; 0.13929	
60	0.06151; *0.12714*	
70	0.05789; 0.08985; 0.11699; *0.12844*; 0.14170	*1.529*(vw)
80	0.04885; 0.09527; *0.12870*	

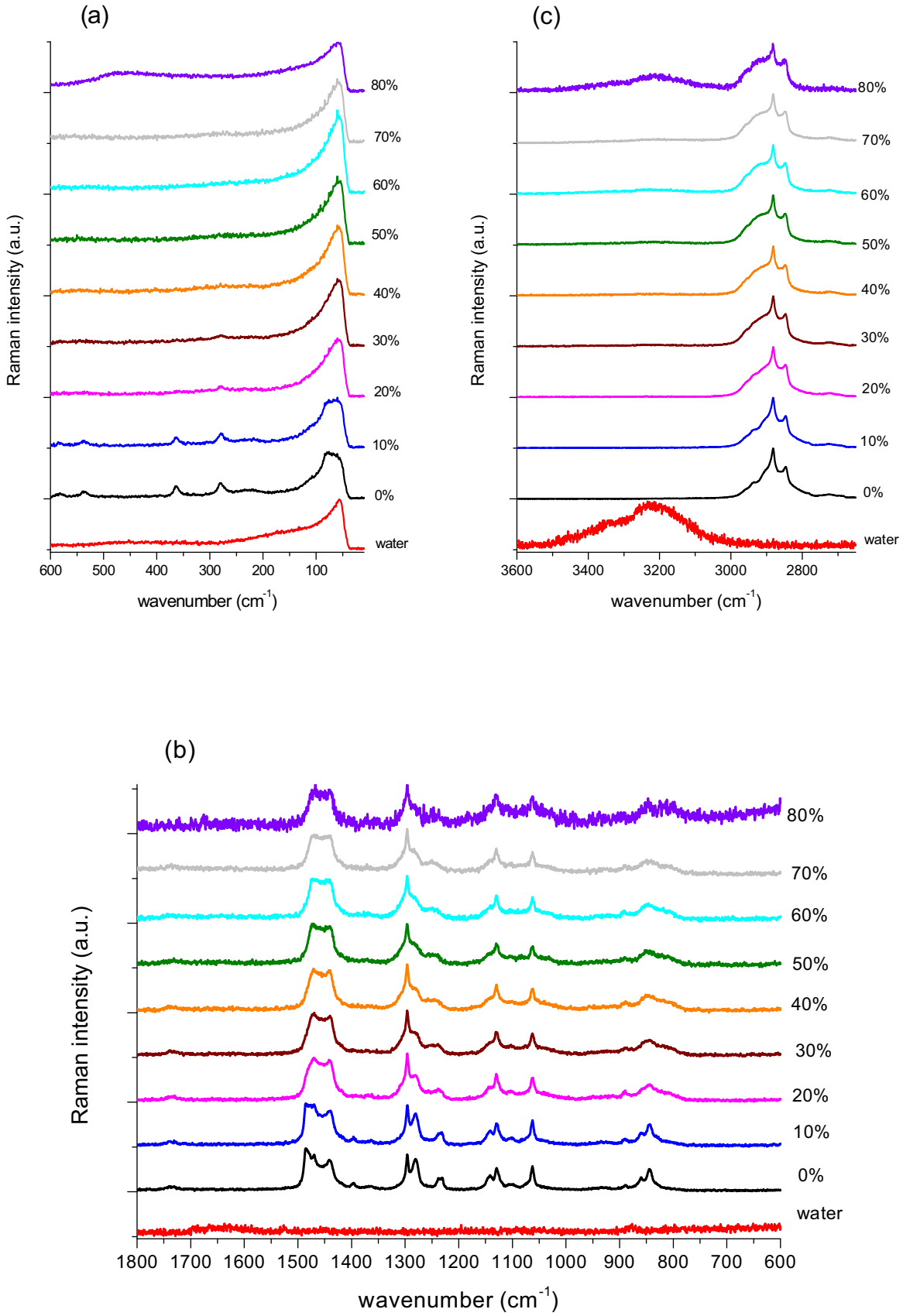

Fig. 2. Raman spectra of Gelucire in the spectral region 600–0 cm^{-1} (a), 1800–600 cm^{-1} (b) and 3600–2700 cm^{-1} (c) as a function of hydration, with an increase from 0% to 80% of water, and with a step of 10%.

et al., 2013). Similarly to these works, the co-existence of two different lamellar phases could be noticed in absence of hydration. Peaks at 0.04823 $Å^{-1}$, 0.09407 $Å^{-1}$ and 0.14352 $Å^{-1}$ correspond to the three-first order of the lamellar phase of the PEG-esters fraction. The d-spacing of this lamellar phase is 131.7 ± 1.7 Å. Peaks at 0.12844 $Å^{-1}$, 0.25814 $Å^{-1}$ and 0.38785 $Å^{-1}$ correspond to the three-first order of the lamellar phase of the glyceride-rich phase. The d-spacing of this second lamellar phase is 48.7 ± 0.2 Å. These two distances are compatible with the reasonable dimensions of the constituting molecules. In the WAXS region, the diffraction peaks at 1.361 $Å^{-1}$ and 1.653 $Å^{-1}$ are the signature of the helical conformation of the PEGs into the Gelucire 50/13. Brubach et al. (2004) state on the influence of the cooling rate on the Gelucire organization. Briefly, a rapid (1 °C/min) or abrupt cooling favors the formation of polymorphic forms with small long periods from 75 to 90 Å while a slowly cooling (0.1 °C/min) favors long lamellar packing without tilt (>120 Å). Regarding our results, it means that the preparation process by evaporation of a chloroformic solution is comparable to a slow cooling process.

After hydration, it is interesting to observe that the SAXS peak corresponding to the first order of the glyceride part of Gelucire 50/13 is not affected by water additions. Indeed, the d-spacing of such lamellar phase fluctuate between 48 and 50 Å ($q \sim 0.12–0.13$ $Å^{-1}$). It is possible that this peak covers diffraction peaks due to the PEG esters mesophases that could explain these slight variations around 0.128 $Å^{-1}$. This result confirms that this lamellar phase is due to the more lipophilic components of Gelucire 50/13, i.e. glycerides. The very weak peak that could be distinguish from the background noise at ~1.5 $Å^{-1}$, in the WAXS region, for some hydration rate (10, 20, 30 and 70%) indicates a hexagonal lateral packing (α) of the acyl chains. The low intensity of this peak strongly suggests the dispersion of this glyceride phase into the samples rather than a phase separation into macroscopic domains.

The whole lyotropic behavior of the PEG ester fraction is more difficult to interpret with the present SAXS data. Hydration rate of 10%, 30%, 70% and 80% seem to give interesting results but 20%, and 40–60% samples are unfortunately poorly informative.

At 10%-hydration, two diffraction peaks, at 0.06452 $Å^{-1}$ and 0.09800 $Å^{-1}$, and a shoulder at 0.03208 $Å^{-1}$ could be observed. They corresponds to the three first order of a lamellar phase having a d-spacing of 194.4 ± 1.8 Å. In the WAXS region, the helical arrangement of the PEG chains totally disappears. These results are coherent with the hydration of the PEG chains which would lead to their disorganization and to an increase of the lamellar period. However, hydration is not enough to significantly modify the packing parameter of the PEG esters and then to induce curvatures in their supramolecular structure.

At 30%-hydration, the diffraction peaks at 0.06573 $Å^{-1}$, 0.08141 $Å^{-1}$, 0.09588 $Å^{-1}$, 0.16282 $Å^{-1}$ and 0.19174 $Å^{-1}$ could be indexed as the reflections at characteristics ratios of $\sqrt{2}$, $\sqrt{3}$, $\sqrt{4}$, $\sqrt{12}$, and $\sqrt{16}$ respectively of a Pn3 m space group with a lattice parameter of 133 ± 2 Å. This corresponds to a Q224 cubic phase. The number of reflection is not very important, probably because Gelucire 50/13 is a complex mixture and not a pure compound but among the most common cubic phases for lipid-based materials, the $\sqrt{2}$, $\sqrt{3}$ and $\sqrt{4}$ set of three is typical of this cubic phase. A ratio of $\sqrt{9}$ would be also typical of this type of phase. Unfortunately, this reflection is covered by the first order of the lamellar phase of the glycerid-rich fraction of Gelucire 50/13. It seems to be same for the $\sqrt{6}$ and $\sqrt{8}$ ratios but it was not possible to deconvolve properly the broad peak at $q \sim 0.12–0.13$ $Å^{-1}$. There is no direct evidence to clarify whether this phase is bicontinuous or micellar. However, its position in the phase diagram, at relatively low hydration rate, suggests it is a bicontinuous structure.

From 40% to 60% hydration, the diffractograms have similar profiles with a weak reflection a low q and a broad peak at $q \sim 0.12–0.13$ $Å^{-1}$. This broad peak certainly masks reflections of the PEG esters phase but it could not be exploited here.

Table 2
Assignments of Raman modes of Gelucire at room temperature; vw = very weak; w = weak; m = medium, s = strong; sh = shoulder; ν = stretching; δ = bending; τ = twisting; ρ = rotation; r = rocking; ω = wagging; s = symmetric; as = asymmetric; T = trans; G = gauche; * = fitted value (El Hadri et al., 2013; Penna et al., 2013; Mounier, 1973; McElmurry et al., 2012).

Raman Frequency (cm^{-1})	Assignment
58 (m)	intermolecular vibration
78 (m)	intermolecular vibration
110 (sh)	intermolecular vibration
219 (w)	δ_s(C—C)
280 (w)	ρ(C—C)
363 (w)	δ_{as}(C—C)
533 (w)	ω(O—H) (PEG 1500)
580 (w)	ω(O—H) (PEG 1500)
845 (m)	$r_{as}(CH_2)$
862 (m)	$r_{as}(CH_2) + \nu$(C—O—C)
891 (w)	ν(C—O—C) (Triglyceride, acyl)
935 (vw)	$r_{as}(CH_2) + \nu$(C—O—C)
1064 (s)	$\nu_{as}(C—C)_T$ (Triglyceride,acyl) + ν(C—O)
1104 (w)	$\nu(C—C)_G$ (Triglyceride, acyl chain)
1130 (s)	$\nu_s(C—C)_T$(Triglyceride, acyl) + $\nu(C—O)_T$
1145 (m)	ν_s(C—C) (Triglyceride, acyl) + $\nu(C—O)_G$
1233 (w)	$\tau_s(CH_2)$ (Triglyceride, acyl) + $\nu(C—O)_T$
1240 (w)	$\tau_{as}(CH_2)$ (Triglyceride, acyl chain)
1282 (s)	$\tau(CH_2)$ (Triglyceride,acyl) + $\nu(C—C)_G$
1298 (m)	$\tau(CH_2)$ (Triglyceride, acyl chain)
1306* (sh)	$\tau(CH_2)$ (Triglyceride, acyl chain)
1400 (vw)	ω(O—H)
1440 (m)	$\delta(CH_2)$
1458* (sh)	$\delta_{as}(CH_3)$
1473* (m)	$\delta(CH_2) + \delta(CH_3)$
1486 (s)	$\delta(CH_3)$ (Triglyceride, acyl) + $\delta(CH_2)$
1738 (w)	ν(C=O) (Triglyceride, acyl chain)
2688 (w)	$\nu(CH_2—CH_2)$
2730 (w)	$\nu(CH_2—CH_2)$
2755 (w)	$\nu(CH_2—CH_2)$
2786 (m)	$\nu(CH_2—CH_2)$
2850 (s)	$\nu_s(CH_2)$
2860* (sh)	$\nu_s(CH_2)$
2882 (s)	$\nu_{as}(CH_2)$
2900* (sh)	$\nu_{as}(CH_2)$
2940 (m)	$\nu_s(CH_3)$ (Triglyceride, acyl chain)
2962* (sh)	$\nu_{as}(CH_3)$ (Triglyceride, acyl chain)

At last, the 70% hydration mixture gives interesting results. Indeed, the diffraction peaks at 0.05789 $Å^{-1}$, 0.08985 $Å^{-1}$, 0.11699 $Å^{-1}$ and 0.14170 $Å^{-1}$ could be indexed as the reflections at characteristics ratios of $\sqrt{2}$, $\sqrt{5}$, $\sqrt{8}$, and $\sqrt{12}$ respectively of a Pm3n space group with a lattice parameter of 153 ± 2 Å. The $\sqrt{5}$ ratio is typical to such cubic phase. Regarding the sequence of ratio, it misses $\sqrt{4}$, $\sqrt{6}$ and $\sqrt{10}$ reflections to perfectly fit the considering space group. However, it should be observed that the reflection corresponding to the $\sqrt{5}$ ratio is broad enough to cover the neighboring peaks. The $\sqrt{10}$ reflection should be at the same position that the first order of the lamellar phase of the glycerid-rich fraction. Even if our data suffer of a lack of resolution at low q-values, such Pm3n, or Q223, cubic phase is reasonable. Because of the high hydration rate, we can also assume that this cubic phase is micellar here.

By considering such Q223 cubic phase, which contains 8 micelles per unit cell, it is possible to do some calculations following developments described and used by authors as Sakya and collaborators (Sakya et al., 1997). The symbols used in the calculations are: M_{esters}, M_{par} and M_{peg}, mean molar mass of whole ester surfactants, paraffinic moiety and PEG moiety; V_{esters}, V_{par} and V_{peg}, mean volume of whole ester surfactants, paraffinic moiety and PEG moiety; ρ_{esters}, ρ_{par} and ρ_{peg}, mean density of whole ester surfactants, paraffinic moiety and PEG moiety. $Ø_{esters}$, $Ø_{par}$ and $Ø_{peg}$, mean volume fraction of whole ester surfactants,

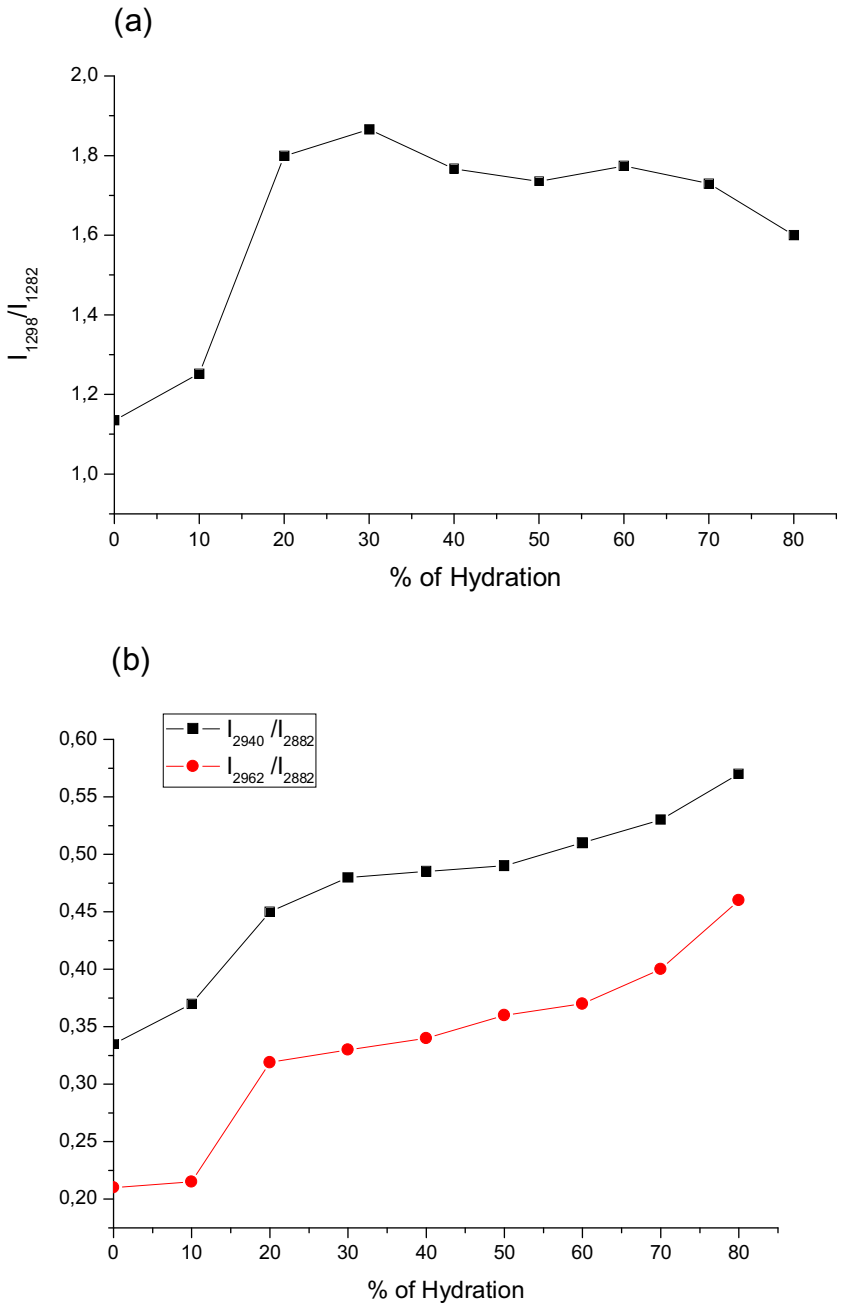

Fig. 3. Variation of intensity ratios of I_{1298}/I_{1282} (a), I_{2940}/I_{2882} and I_{2962}/I_{2882} (b) as a function of rate of hydration of Gelucire 50/13.

paraffinic moiety and PEG moiety. Mean values have been calculated by taking into account the composition of Gelucire 50/13 proposed by Brubach et al. (2004). Applied to the mean HLB calculation thanks to the Griffin method, this approach leads to a HLB of 13 as given by the supplier. ρ_w is the water density, *a*, the lattice parameter, *c*, the weight fraction of surfactant (compared to water) and *n*, the number of micelles per unit cell. Here, after exclusion of the non-PEG ester fractions of the Gelucire 50/13, the weight fraction of surfactant compared to water, *c*, is 0.31.

The volume fractions of whole surfactant and of paraffin chain (lipid part) are given by the following equation respectively:

$$\Phi_{esters} = \left(1 + \frac{\rho_{esters}(1-c)}{\rho_w c}\right)^{-1} \quad (1)$$

$$\Phi_{par} = \left(1 + \frac{M_{peg}\rho_{par}}{M_{par}\rho_{peg}} + \frac{M_{esters}\rho_{par}(1-c)}{M_{par}\rho_w c}\right)^{-1} \quad (2)$$

For PEG mono- and diesters constituting Gelucire 50/13, the mean molar masses M_{esters}, M_{par} and M_{peg} are respectively 1895, 382 and 1513 g/mol. Taking the volumes of CH_2/CH_3, CH_2CH_2OH and OH groups to be 27, 61 and 17 Å^3, respectively, the corresponding volumes, V_{esters}, V_{par} and V_{peg} are 2808, 734 and 2074 Å^3. Hence the densities ρ_{esters}, ρ_{par} and ρ_{peg} are 1.121, 0.864 and 1.211 g/cm^3.

Incorporating each value into Eqs (1) and (2), it is possible to calculate $Ø_{esters}$ and $Ø_{par}$ equal to 0.285 and 0.074 respectively. If we hypothesize that micelles are spherical, the radius of either the

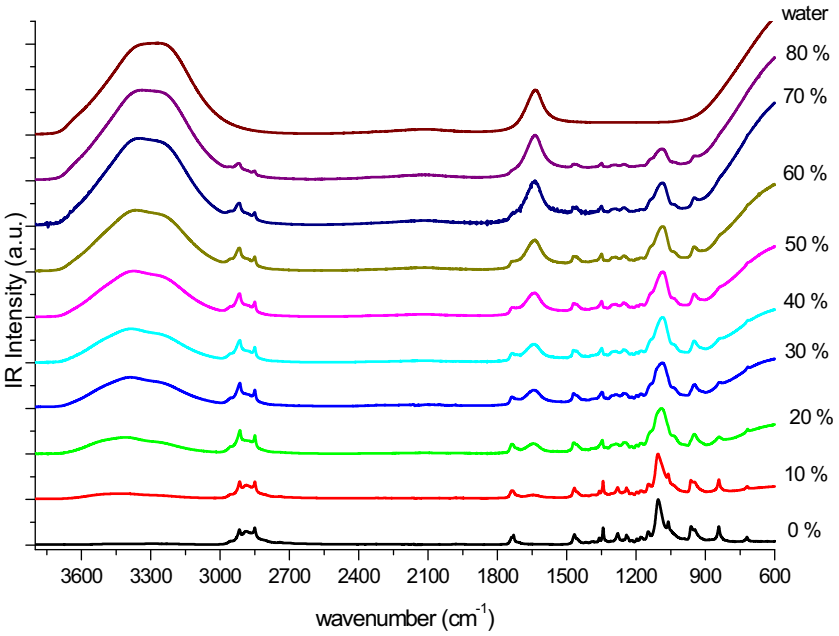

Fig. 4. IR spectra of Gelucire in the spectral region 3900–600 cm^{-1} as a function of hydration, with an increase from 0% to 80% of water, and with a step of 10%.

lipid core or the micelle, r_{par} and r_{esters} respectively, is given by the generalized equation:

$$r_x = \left(\frac{3a^3\Phi_x}{4\pi n}\right)^{1/3} \quad (3)$$

The area per molecule at the polar – non polar interface, *s*, and the mean number of molecule per micelles, N, are respectively:

$$s = \frac{3v_{par}}{r_{par}} \quad (4)$$

$$N = \frac{4\pi r_{par}^2}{s} \quad (5)$$

Thus, it results from all the calculations that the mean radius of the micelles, r_{esters}, is ~32 Å with a radius of the lipid inner core, r_{par}, ~20 Å. The aggregation number is ~46 molecules. Interestingly, the radius of the core is compatible with the expected chain length of 16 and 18 carbons that could be calculate between 20 and 23 Å. On the contrary, the PEG layer seems underestimate compared to what we should expect from classical mushroom and brush models applied to a chain containing a mean of 34 EO units that should be ~40 Å. The first reason is that the most important proportion of PEG esters in Gelucire 50/13 are diesters, meaning that fatty acids are branched at both extremities of the PEG chains. This leads to a double anchorage of the esters into the lipid core, a decrease of the degree of freedom of the polymer part and then to discrepancies compared to the models. The second reason could be the limitation of the spherical model applied in our calculation. Indeed, several authors have shown that the Pm3n micellar cubic phase contains more than one kind of structural element (Tardieu and Luzzati, 1970; Fontell et al., 1985). More precisely, the co-existence of two spherical and six disk-shaped micelles per unit cells have been proposed by Charvolin and Sadoc (1988). The co-existence of two different types of micelles is very seducing for Gelucire 50/13 as the packing parameter of the monoesters and diesters are certainly different and could be at the origin of segregations. The hypothesis here is that the monoesters, certainly having low packing parameter, will generate more spherical objects than diesters which have a more voluminous hydrophobic tail and then a higher packing parameter.

3.1. Raman spectroscopy study

To confirm and complete the study of structural changes of Gelucire 50/13 as a function of the rate of hydration, we will focus this time our research on vibrational behavior of Gelucire 50/13 hydrated by Raman spectroscopy. We presented in Fig. 2a–c, the Raman spectra of the Gelucire 50/13 as a function of hydration in the spectral range respectively 600–10, 1800–600 and 3600–2700 cm^{-1}, with an increase from 0% to 80% of water and with a step of 10%. From this figures, we notice many changes of vibrational behavior in two spectral regions: 1800–10 and 3600–2650 cm^{-1}. To facilitate the study, we will present the results obtained using these two spectral regions.

3.1.1. In the spectral region 1800–10 cm^{-1}

In this spectral region, a large number of peaks are observed: 59, 78, 110, 219, 280, 363, 533, 580, 845, 862, 891, 935, 1064, 1104, 1130, 1145, 1233, 1240, 1282, 1298, 1306, 1400, 1440, 1458*, 1473*, 1486* and 1738* cm^{-1}. The frequency values indexed by * are fitted values (Curve fitting was performed as per Bresson et al. (2006)) (Table 2).

We presented in Fig. 2a, the Raman spectra of the Gelucire 50/13 as a function of hydration in the spectral region 600–10 cm^{-1}. We see that the modes at 110, 219, 363, 533 and 580 cm^{-1} disappears rapidly from 10% hydration, while the mode 280 cm^{-1} disappears from 30% hydration. Moreover, we note that the vibrational mode at 78 cm^{-1} to intermolecular interactions (McElmurry et al., 2012) corresponds to a resolved peak from 0% to 10% of hydration whereas after 20% of hydration we observe only a shoulder.

For 0% and 10% of hydration, we observe a resolved doublet at 860 and 845 cm^{-1}. From 20% of hydration, this doublet is transformed into a wide peak centered on 845 cm^{-1} with two shoulders one at 810 cm^{-1} and the other one at 860 cm^{-1}. At the same time, from 20% of hydration the resolved doublet at 1145 and

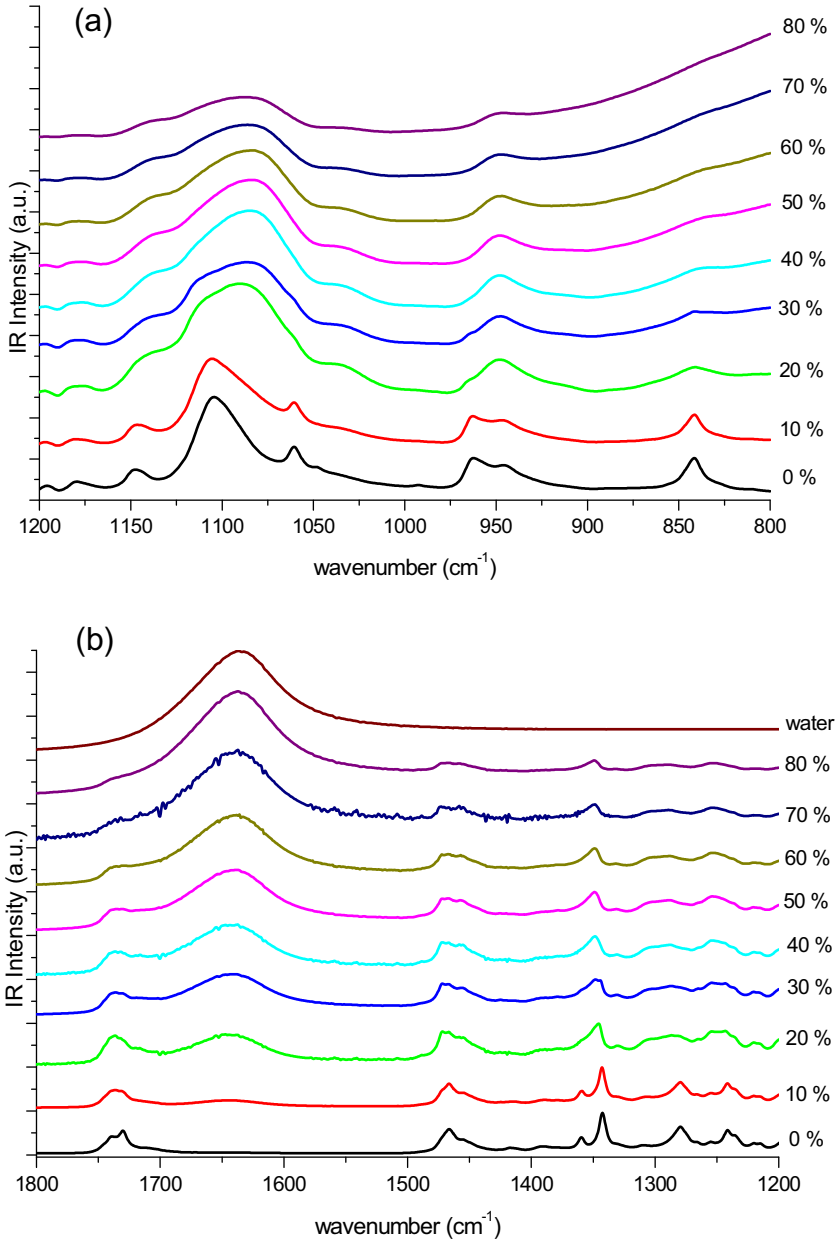

Fig. 5. IR spectra of Gelucire in the spectral region 1200–600 cm^{-1} (a) and in the band 1200–1000 cm^{-1} (Effect of hydrogen bonding) as a function of hydration.

1130 cm^{-1} becomes an unresolved doublet with a weakening in intensity of the peak at 1145 cm^{-1} assigned to ν_s(C—C) (Triglyceride, acyl) + ν(C—O)$_G$.

To assess the impact of hydration on the Gelucire 50/13 in the spectral region1800–600 cm^{-1} (Fig. 2b), we studied the intensity ratio I_{1298}/I_{1282} between the mode 1298 cm^{-1} assigned to the CH_2 twisting involved in triglycerides and the acyl chains of MPEG and DPEG, and the mode at 1282 cm^{-1} assigned to both of the torsion of CH_2 involved in triglycerides and the acyl chains of MPEG and DPEG and *gauche* stretching vibration of the C—C bond. On Fig. 3a, we present the variation of this ratio as a function of hydration. As a function of the rate of hydration, we observe for the intensity ratio I_{1298}/I_{1282} a sharp increase between 0% and 20% hydration (up from 1.1 to 1.8) then a relative stagnation until 80% of hydration.

In the spectral region 1500–1400 cm^{-1} characterized by the vibrational modes of CH_2, CH_3 bending, we observe that from 20% of hydration the mode at 1486 cm^{-1} assigned to $\delta(CH_3)$ (Triglyceride, acyl) + $\delta(CH_2)$ seems to decrease strongly in intensity. Thus, we find that the variations of the intensity ratios I_{1298}/I_{1282} and of the intensity of the mode at 1486 cm^{-1} according to hydration is a marker conformational changes in the Gelucire as was the case in studies of Gelucire as a function of the temperature (El Hadri et al., 2013, 2015) by Raman spectroscopy and X-ray diffraction.

All these changes seem to confirm that after 10% of hydration the helical structure of PEG seems to disappear.

3.1.2. In the spectral region 3600–2650 cm^{-1}

In the second spectral region, characterized by the stretching vibrations of C—H, some peaks can be easily pointed, others not. In total, in region 3600–2650 cm^{-1}, we were able to determine 9 different modes: 2688, 2730, 2755, 2786, 2850, 2882, 2890*, 2940* and 2962* cm^{-1}. On Fig. 2c, we present the Raman spectra of the Gelucire as a function of hydration in the spectral region 3600–2650 cm^{-1}. As the region 1800–10 cm^{-1}, this region also has peaks which appear to vary significantly depending on the hydration:

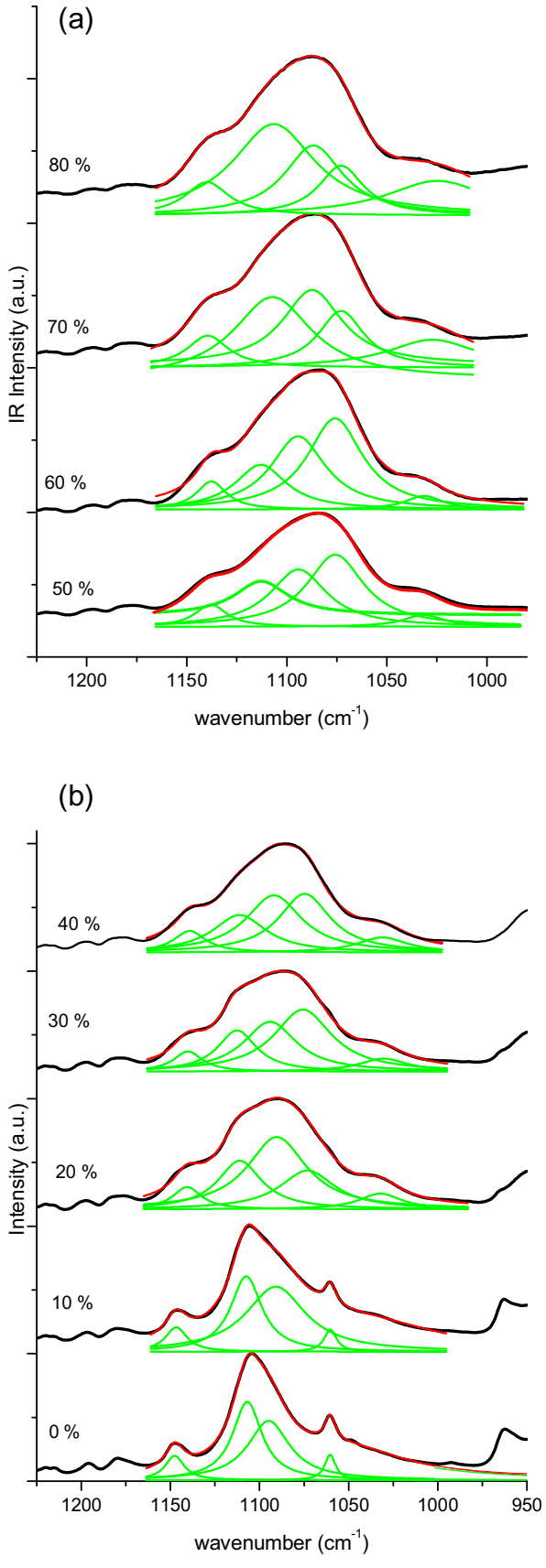

Fig. 6. IR spectra of Gelucire 50/13 fitted by Lorentzian curves as a function of hydration in the spectral region 1250–950 cm^{-1} (b) from 0% to 40% of hydration and (a) from 50% to 80% of hydration.

modes at 2940 and 2962 cm^{-1} assigned to $\nu_s(CH_3)$ and $\nu_{as}(CH_3)$ (Triglyceride, acyl chain) respectively.

Based on these spectra, we observe changes in intensity between the vibrational modes at 2850, 2882, 2940 and 2962 cm^{-1}. The intensity variations observed for these vibrational modes are also direct witnesses of mobility twisting-rotations of individual chains of PEG 1500, MPEG, DPEG and triglycerides. To evaluate this mobility and as in the study of Gelucire as a function of the temperature (El Hadri et al., 2013, 2015), we present the variations of two intensity ratios $I\nu_s(CH_3)/I\nu_{as}(CH_2) = I_{2940}/I_{2882}$ and $I\nu_{as}(CH_3)/I\nu_s(CH_2) = I_{2962}/I_{2882}$ but this time as a function of the hydration on Fig. 3b.

On Fig. 3b, the two intensity ratios seem to have the same evolution: a fast rise between 0% and 20% then a slower increase between 20% and 60% and again a more significant rise of the ratio. The ratio $I\nu_s(CH_3)/I\nu_{as}(CH_2) = I_{2940}/I_{2882}$ passes from 0.33 to 0.57. In the same time, $I\nu_{as}(CH_3)/I\nu_s(CH_2) = I_{2962}/I_{2882}$ passes from 0.21 to 0.46. The modes at 2940 and 2962 cm^{-1} are linked to CH_3 which it sensitive to the phase change. As in the study as a function of the temperature (El Hadri et al., 2013, 2015), the more we approached the melting temperature of the Gelucire, more the intensity of this peak grew. This is also the case here as a function of the rate of hydration. This ratio is therefore a marker of structural changes in the water-Gelucire mixture. This marker is particularly sensitive here during the passage from the lamellar phase to the cubic phase of PEG after 20% hydration.

3.2. Study in infrared spectroscopy

We presented in Fig. 4 the IR spectra of the Gelucire 50/13 as a function of hydration in the spectral range 3700–600 cm^{-1}, with an increase from 0% to 80% of water and a step of 10%, obtained by ATR/FTIR. From this figure, we notice changes in behavior in three spectral ranges: 1200–600, 1800–1200 and 3600–2700 cm^{-1}. Indeed, we note the appearance of a peak at 1645 cm^{-1} and a wide band centered around 3385 cm^{-1} assigned to the water bands (ν(O—H) and δ(O—H)). The intensity of these modes increases with the rate of hydration of Gelucire. The C=O stretching modes and CH_2 bending modes in the spectral range 1500–1400 cm^{-1} seem not to change significantly according the rate of hydration. In contrary to the spectral range 1800–1000 cm^{-1}, the two spectral ranges 1400–1300 and 1200–1000 cm^{-1} are more sensitive to the rate of hydration as can be seen on Fig. 5a and b.

3.2.1. In the spectral region 1200–600 cm^{-1}

In Fig. 6, we present the IR spectra of Gelucire 50/13 adjusted by Lorentzian functions according to the rate of hydration in the spectral region 1250–950 cm^{-1}. We observe important changes on this figure from 20% of hydration and from 70% of hydration. From 20% of hydration, we observe the appearance of a peak at 1031 cm^{-1} assigned in $r(CH_2)$ and a weakening in intensity of the peak at 960 cm^{-1}. At the same time, three vibrational modes vary significantly: the mode at 1060 cm^{-1} shifts to 1075 cm^{-1} from 20% of hydration (+15 cm^{-1}), the mode at 1107 cm^{-1} to 1112 cm^{-1} (+5 cm^{-1}) and the mode at 1147 cm^{-1} to 1140 cm^{-1} (−5 cm^{-1}). Concerning the intensity of these modes, we remark that the intensity of the modes at 1095, 1145 and 1031 cm^{-1} seem to be constant more or less whereas the intensity of the mode at 1112 cm^{-1} decreases and the mode at 1075 cm^{-1} rises in intensity according to the rate of hydration. But, whereas from 20% to 60% of hydration the peaks at 1031, 1075 and 1112 cm^{-1} seem to have the same behavior intensity, from 70% of hydration, we observe a new shift between peaks at 1075 and 1112 cm^{-1}: the intensity of the peak at 1112 cm^{-1} becomes again more important than that of the peak at 1075 cm^{-1}. This behavior intensity of these three modes seems similar to that obtained for the cases in 0% and 10% of

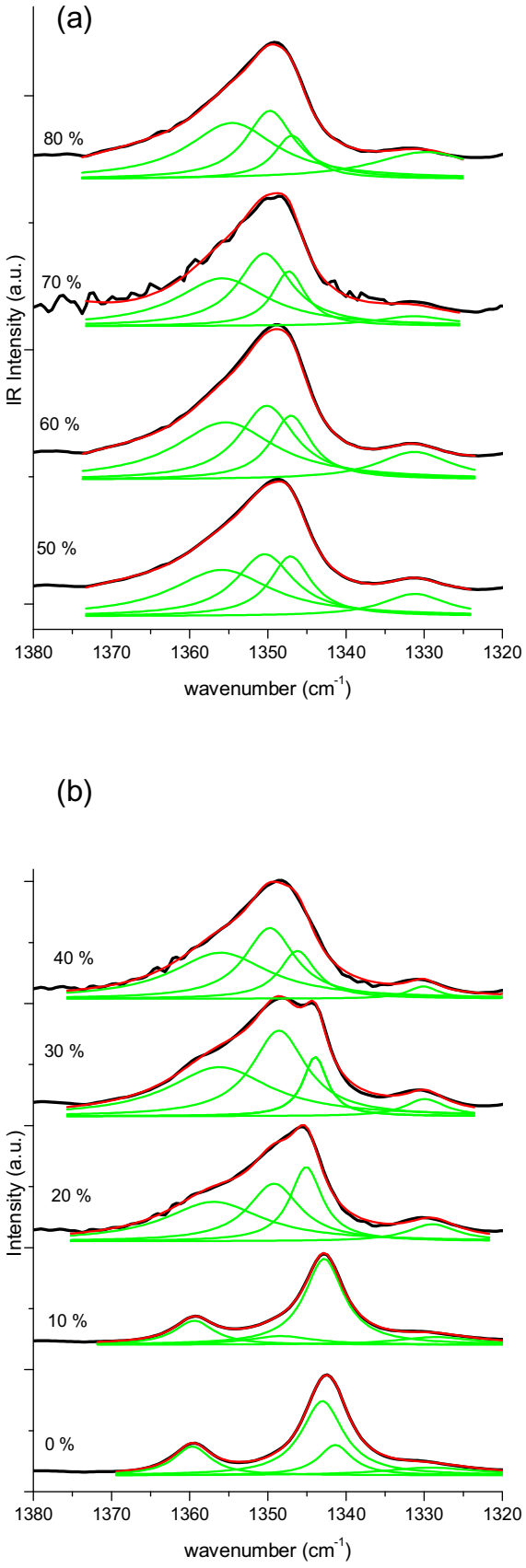

Fig. 7. IR spectra of Gelucire 50/13 fitted by Lorentzian curves as a function of hydration in the spectral region 1380–1320 cm^{-1} (b) from 0% to 40% of hydration and (a) from 50% to 80% of hydration .

hydration but the global envelope of the spectrum is different what lets us think that the molecules of Gelucire are not in the same arrangement.

Rozenberg et al. (1998) show that in IR spectroscopy the most noticeable changes for hydrated PEG-200 are observed for the wavenumber position and width of the components near 1068, 1104 and 1127 cm^{-1} assigned above to ν(C—OH), $\nu(C—O)_{trans}$ and $\nu(C—O)_{gauche}$ respectively at the water/PEG ratios 0.5:1.5. As for the intensities, while the total integrated band intensity is essentially constant, one notes a progressive increase of the 1104 cm^{-1} component (*trans* conformation) and a corresponding decrease of the 1126 cm^{-1} component (*gauche* conformation) with higher water concentration evident in the parallel growth of the water band near 1650 cm^{-1}. The changing ratio between the two conformations is the result of the whole H-bond structure changing when water molecules integrate into it. Water molecules have the effect of increasing the length of the H-bonded chain, letting the system to preferably relax to the energetically favored *trans* conformations. In contrast, the smallest changes are of the components near 1031 and 1142 cm^{-1} assigned to stretching (C—C) vibrations and deformational vibrations of ($—CH_2—$) groups. The most significant conclusion is that the changes of the parameters of the 1068 cm^{-1} component, assigned to ν(C—OH), strongly indicate the participation of the OH-group in this process of water molecules joining the H-bond system of the PEGs (Rozenberg et al., 1998). Furthermore, Begum and Matsuura (1997) showed that the gauche state of the C—C bond, which is typical for the crystalline helical state, is retained when PEG is dissolved in water. Applied tension could drive a transition from a helix to an all-trans configuration, energetically less favorable in the absence of strain.

So, from these results, it seems that we observe the same phenomenon in the case of the hydrated Gelucire 50/13 but with frequency shifts for the modes assigned to ν(C—OH), $\nu(C—O)_{trans}$ and $\nu(C—O)_{gauche}$. For the Gelucire 50/13, the peak at 1075 cm^{-1} can be assigned to ν(C—OH) (+7 cm^{-1} in comparison with Rozenberg's results), the peak at 1095 cm^{-1} assigned to $\nu(C—O)_{trans}$ (−9 cm^{-1}) and the peak at 1112 cm^{-1} assigned to $\nu(C—O)_{gauche}$ (−14 cm^{-1}). The increase in intensity of the ν(C—OH) vibrations and the decrease of the contribution of $\nu(C—O)_{gauche}$ vibrations for the Gelucire 50/13 according the rate of hydration seem to indicate that water molecules tend to join the existing hydrogen bonded structure of PEGs at the hydroxyl end groups.

3.2.2. In the spectral region 1800–1200 cm^{-1}

If we focused on the spectral region 1400–1300 cm^{-1}, we can observe from Fig. 7 similar changes from 20% rate of hydration. In the spectral region 1400–1300 cm^{-1}, we notice that one vibrational mode at 1349 cm^{-1} appears from 10% of hydration. At the same time, two vibrational modes vary slightly: the mode at 1342 cm^{-1} shifts to 1345 cm^{-1} from 20% of hydration (+3 cm^{-1}), the mode at 1360 cm^{-1} to 1356 cm^{-1} (−4 cm^{-1}). The mode at 1330 cm^{-1} seems to vary very slightly. Concerning the intensity of these modes, we remark that the intensity of the modes at 1330 and 1356 cm^{-1} seem to be constant more or less whereas the intensity of the mode at 1344 cm^{-1} decreases and the mode at 1349 cm^{-1} rises in intensity according to the rate of hydration.

Begum and Matsuura (1997) showed that the relative population of the *gauche* conformation around the C—C bond increases significantly with increasing water fraction in PEGs whereas the *trans* conformation around C—O bond increases. Furthermore, Naik and Vasudevan (2011) indicate that the CH2 wagging modes in the IR spectrum between 1170 and 1380 cm^{-1} progress when temperature increase. It seems to indicate that *trans* conformers are dominant in the methylene chain. In comparison with our results, it will seem that in this spectral region, the mode at

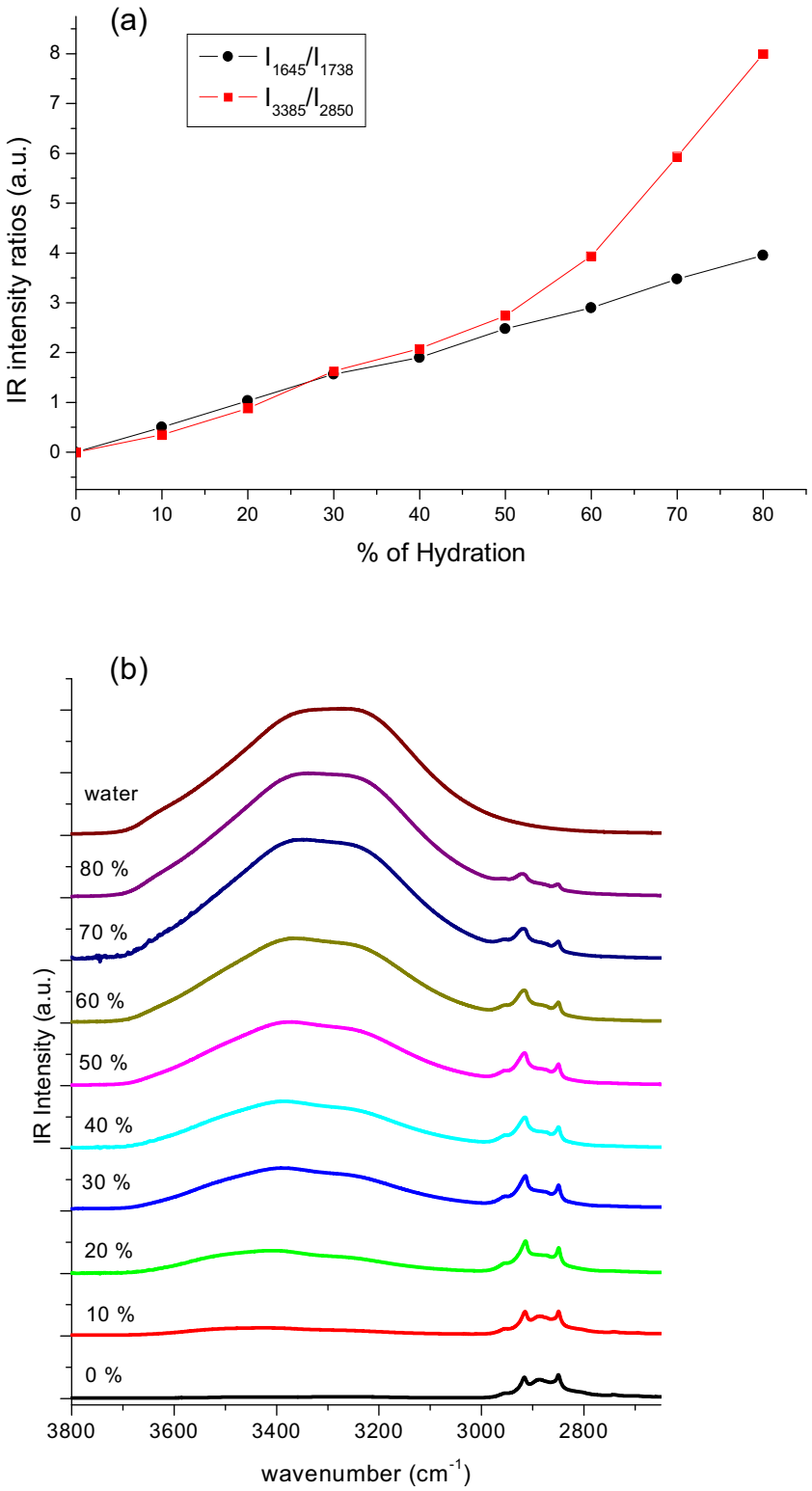

Fig. 8. Variation of intensity ratios of I_{3385}/I_{2850} and I_{1645}/I_{1738} (a) and IR spectra of Gelucire in the spectral region 3800–2700 cm^{-1} (b) as a function of hydration.

1344 cm^{-1} can be dominated by the $\nu(C—O)_{gauche}$ vibrations and the peak at 1349 cm^{-1} to the CH_2 wagging vibrations.

Finally, in the region 1760–1600 cm^{-1}, we observe the appearance of a mode at 1635 cm^{-1} assigned to δ(OH) at 10% hydration which will predominate in intensity throughout this spectral region during increasing the rate of hydration. On Fig. 8a), we present the variations of the intensity ratio Iδ (O—H)/Iν(C=O) = I_{1645}/I_{1738} according to the rate of hydration. This intensity ratio is quadrupled between 0% and 80% a regular rise. We note also in this region a change of the vibrational behavior of carbonyl groups (C=O): at 0% hydration, we have a resolved doublet with a shoulder (3 components) whereas from 10%, we observe a broad peak. It is

Table 3
Assignments of IR modes of Gelucire at room temperature; vw = very weak; w = weak; m = medium, s = strong; sh = shoulder; ν = stretching; δ = bending; τ = twisting; ρ = rotation; r = rocking; ω = wagging; s = symmetric; as = asymmetric; T = trans; G = gauche; * = fitted value (Brubach et al., 2004; Colthup et al., 1990; Kozielski et al., 2005; Bresson et al., 2011).

IR frequency cm^{-1}	Assignment
719 (w)	$r(CH_2)$
841 (m)	$r_{as}(CH_2)$
946 (m)	$r(CH_2)$
961 (m)	$r_s(CH_2)$
1038 (sh)	$r_s(CH_2)$
1060 (m)	$\nu_{as}(COC) + r_s(CH_2)$
1095 (sh)	$\nu(C—C) + \nu(C—O) + r(CH_3)$
1107 (vs)	$\nu(C—C) + \nu(C—O) + r(CH_3)$
1147 (m)	$\nu(C—C) + \nu(C—O) + r(CH_3)$
1177 (w)	$\nu(C—C) + \nu(C—O) + r(CH_3)$
1196 (vw)	
1219 (vw)	
1240 (m)	$\tau_s(CH_2)$ $\tau_{as}(CH_2)$
1279 (m)	$\tau(CH_2)$
1306 (vw)	$\tau(CH_2)$
1330 (sh)	$\nu(C—C)_T + \omega(CH_2)$
1342 (m)	$\omega(CH_2)$tggt
1360 (w)	$\omega(CH_2)$tggt
1385 (vw)	$\omega(O—H)$
1415 (vw)	$\delta(O—CH_2)$
1454 (w)	$\delta(CH_2)$
1465 (m)	$\delta(CH_2)$
1645 (m)	$\delta(O—H)$
1735 (m)	$\nu(C=O)$
2700 (w)	$\nu(CH_2—CH_2)$
2741 (w)	$\nu(CH_2—CH_2)$
2812* (w)	$\nu_s(CH_2)$
2850 (s)	$\nu_s(CH_2)$
2857* (w)	$\nu_s(CH_2)$
2878* (w)	$\nu_{as}(CH_2)$
2889 (s)	$\nu_{as}(CH_2)$
2917 (s)	$\nu_{as}(CH_2)$
2925 (sh)	$\nu_s(CH_3)$
2956 (w)	$\nu_{as}(CH_3)$
3455 (w)	$\nu(O—H)$

remarked that in this region there is an effect of hydrogen bonding and especially in the band 1750–1700 cm^{-1}, where we observe a shift of the C=O mode from 1735 to 1745 cm^{-1} (Fig. 5b) (Pesvner and Die, 2001).

3.2.3. In the spectral region 3600–2600 cm^{-1}

In Fig. 8b, we present the IR spectra of the Gelucire 50/13 as a function of hydration in the spectral range 3900–2600 cm^{-1}. In this figure, it is observed that hydration has a large influence on the spectrum of Gelucire on the one hand, with the appearance of a broad peak assigned to stretching OH associated to water in the band 3500–3200 cm^{-1} which increases in intensity very significantly until absorb in intensity the spectral region related to vibrational modes of valence of the CH bonds centered on 2900 cm^{-1}, and in the other hand, with the shift of CH stretching bands due to the effect of hydrogen bond, which it move to bases frequencies (high wavelengths) and it's accompanied by enlargements of elongation bands CH, CH_2 and CH_3 of the spectral region 3000–2700 cm^{-1} (Fig. 8b) (Silverstein et al., 1998). Also, we observe that some vibrational modes disappear after 10% hydration, this is the case of modes 2700, 2741 assigned to $\nu(CH_2—CH_2)$, and 2812, 2860 cm^{-1} assigned respectively to $\nu_s(CH_2)$ and $\nu_{as}(CH_2)$.

For the spectral region corresponding to the modes of stretching ν(O—H), we present in Fig. 8a the intensity ratio I_{3385}/I_{2850} to show the very significant change in the intensity of these modes as a function of the rate of hydration. There is a variation of the ratio from 0 to 8, with two fast rise from 0% to 20% of hydration and from 60% to 80% of hydration. This region is quite a privileged indicator of the effect of water on the Gelucire 50/13: lamellar period between 0% and 10% of hydration, bicontinuous structure between 20%–70% and from 70% of hydration micellar phase (Table 3).

4. Conclusion

In this work, we have characterized the structural and vibrational changes of Gelucire as a function of the rate of

Table 4
Summary of changes in functional group band intensity according to the degree of hydration. ↑/↓ = weak; ↑↑/↓↓ = moderate; ↑↑↑/↓↓↓ = strong changes; "=" = stable; φ = non-existent.

Group	Location (cm^{-1})	Spectroscopy	Lamellar phase *0%–10%*	Bicontinuous Struture *20%–60%*	Micellar phase *70%–80%*
ν(O—H)	≈3385	IR	ϕ	↑↑	↑↑↑
$\nu_{as}(CH_3)$	2962	Raman	↑↑	=	↑↑
$\nu_{as}(CH_3)$	2940	Raman	↑↑	=	↑
$\nu_s(CH_2)$	2860	IR	=	ϕ	ϕ
$\nu_s(CH_2)$	2812	IR	=	ϕ	ϕ
$\nu(CH_2—CH_2)$	2741	IR	=	ϕ	ϕ
$\nu(CH_2—CH_2)$	≈2700	IR	=	ϕ	ϕ
δ(O—H)	1645	IR	ϕ	↑↑	↑↑
$\delta(CH_3) + \delta(CH_2)$	1486	Raman	↓↓	=	=
$\omega(CH_2)$	≈1349	IR	ϕ	↑↑	=
ω (CH_2)	≈1342	IR	=	↓	=
ω (CH_2)	1330	IR	=	↑	=
τ (CH_2)	1280	Raman	↓↓	=	=
(C—C) + ν(C—O)	1145	Raman	=	↓	↓
ν(C—C) + ν(C—O)	≈1107	IR	=	↓↓	↑↑
ν(C—O—C)	≈1060	IR	=	↑↑	↓↓
$r(CH_2)$	1031	IR	ϕ	↑	=
$r(CH_2)$	961	IR	=	↓↓	=
$r(CH_2)$	946	IR	=	↑↑	=
$r(CH_2)$	862	Raman	=	↓	↓
$r(CH_2)$	810	Raman	=	↑	↑
δ(C—C)	363	Raman	=	ϕ	ϕ
ρ(C—C)	280	Raman	=	ϕ	ϕ
intermolecular	110	Raman	=	ϕ	ϕ

hydration by X-ray diffraction, Infrared spectroscopy and Raman spectroscopy. The study by X-ray diffraction showed that the structure of Gelucire depends strongly on the hydration which resulting by the successive passage of a structure to another:

- Between 0% and 10%: a lamellar structure of PEG.
- Between 20% and 70%: a bicontinuous structure.
- Between 70% and 80%: a micellar phase.

From these results in X-ray diffraction, we have studied the Gelucire 50/13 as a function of the rate of hydration in FTIR and Raman spectroscopy in order to know whether the structural changes observed in X-ray diffraction were also visible at the point of view vibrational. Notably, changes in key functional group band intensity during the structure transitions according to the rate of hydration were observed and are summarized in Table 4.

At the infrared spectroscopy study, we obtained spectra in the spectral region 4000–600 cm^{-1}. In spectral regions 1200–600, 1800–1200 and 3600–2600 cm^{-1}, many vibrational modes were found to be important witnesses of structural changes observed in X-ray diffraction. These vibrational changes are manifested by shifts in frequency, significant variations in the intensity and the appearance or disappearance of vibrational modes from a precise value of the rate of hydration. The vibrational modes assigned to ν(O—H) at 3385 cm^{-1}, to ν(C—OH) at 1075 cm^{-1} and to $\nu(C—O)_{gauche}$ at 1112 cm^{-1} seem to be the most sensitive to three changes of structure. The others modes assigned to $\nu_s(CH_2)$ at 2860 and 2812 cm^{-1}, to $\omega(CH_2)$ at 1349, 1342 and 1330 cm^{-1}, and $r(CH_2)$ at 1031, 960 and 946 cm^{-1} have two different vibrational behaviors following the rate of hydration. In most cases, the changes occurred after 10% rate of hydration.

In Raman spectroscopy, compared to IR spectroscopy, we have a broadening of the spectrum: the spectral range becomes from 4000 to 45 cm^{-1}, showing a region at low frequencies (300–45 cm^{-1}) where we found a modes vibrational linked with inter and intramolecular interactions. In other bands, we observed similar changes to those noted in IR spectroscopy but for a smaller number of modes. The vibrational modes which are the most sensitive to the variations of rate of hydration are the modes $\nu_{as}(CH_3)$ assigned to 2962 and 2940 cm^{-1}. Nevertheless, in Infrared where we observe the higher impact of the addition of water via the modes linked to bonds O—H, δ(O—H) and ν(O—H). These results in Raman spectroscopy and IR were consistent with the other results of Gelucire in function of the temperature (El Hadri et al., 2013) and RX.

Conflict of interest

The authors declares no conflict of interest.

Acknowledgments

We would like to thank Heinz Amenitsch (Austrian SAXS Beamline, Elettra, Trieste) for his support during the SAXS-WAXS experiments and Quentin Arnould, technician of *Walloon Agricultural Research Centre (CRA-W)*, who participated to ATR-FTIR and FT-Raman measurements.

References

Begum, R., Matsuura, H., 1997. Chem. Soc. Faraday Trans. 93 (21), 3839–3848.
Bresson, S., El Marssi, M., Khelifa, B., 2006. Vib. Spec. 40, 263–269.
Bresson, S., Rousseau, D., Ghosh, S., El Marssi, M., Faivre, V., 2011. Eur. J. Lipid Sci. Technol. 113 (8), 992–1004.
Brubach, J.B., Ollivon, M., Jannin, V., Malher, B., Bourgaux, C., Lesieur, P., Roy, P., 2004. J. Phys. Chem B 108, 17721–17729.
Charvolin, Sadoc, 1988. J. Phys. 49, 521–526.
Colthup, N.B., Daly, L.H., Wiberley, S.E., 1990. Introduction to Infrared and Raman Spectroscopy, 3rd edition Academic Press Limited, London.
Craig, D.Q.M., Newton, J.M., 1991. Int. J. Pharm. 74, 33–41.
Da Silva, E., Bresson, S., Rousseau, D., 2009. Chem. Phys. Lipids 157, 113–116.
Damian, F., Blaton, N., Naesens, L., Balzarini, J., Kinget, R., Augustijns, P., Van den Mooter, G., 2000. Eur. J. Pharm. Sci. 10, 311–322.
El Hadri, M., 2013. Vib. Spectrosc. 64, 78–88.
El Hadri, M., 2015. J. Mol. Struct. 1083, 441–449.
Fontell, 1985. Mol. Cryst. Liq. Cryst. Lett. 1, 9–17.
Gines, J.M., Veiga, M.D., Arias, M.J., Rabasco, A.M., 1995. Int. J. Pharm. 126, 287–291.
Gupta, M.K., Goldman, D., Bogner, R.H., Tseng, Y.C., 2001. Pharm. Dev. Technol. 6, 563–572.
Hu, Y.R., Liang, J.K., Myerson, A.S., Taylor, L.S., 2005. Ind. Eng. Chem. Res. 44, 1233–1240.
Jannin, V., Rodier, J.-D., Musakhanian, J., 2014. Int. J. Pharm. 466, 109–121.
Kozielski, M., Mühle, M., Błaszczak, Z., Szybowicz, M., 2005. Cryst. Res. Technol. 40 (4/5), 466–470.
McElmurry, B.A., Rivera-Rivera, L.A., Scott, K.W., Wang, Z., Leonov, I.I., Lucchese, R.R., 2012. Chem. Phys. 409, 1–10.
Mounier, J., 1973. J. Organomet. Chem. 56, 67–77.
Mouricout, A.M., Gerbaud, D., Brossard, C., Lefort des Ylouses, D., 1990. S.T.P. Pharm. 6, 368–375.
Naik, V.V., Vasudevan, S., 2011. J. Phys. Chem. C 115, 8221–8232.
Penna, T.C., Faria, L.F.O., Matos, J.R., Ribiero, M.C.C., 2013. J. Chem. Phys. 138, 104503.
Perissutti, B., Rubessa, F., Princivalle, F., 2000. S.T.P. Pharm. Sci. 10, 479–484.
Pesvner, A., Die, M., 2001. Appl. Spectrosc. 55 (6), 788–793.
Pivette, P., Faivre, V., Mancini, L., Gueutin, C., Daste, G., Ollivon, M., Lesieur, S., 2012. J. Controlled Release 158 (3), 392–402.
Qi, S., Belton, P., McAuley, W., Codoni, D., Darji, N., 2013. Pharm. Res. 30 (4), 1123–1136.
Rosiaux, Y., Jannin, V., Hughes, S., Marchaud, D., 2014. J. Controlled Release 188, 18–30.
Rozenberg, M., Loewenschuss, A., Marcus, Y., 1998. Spectrochim. Acta Part A 54, 1819–1826.
Sakya, P., Seddon, J.M., Templer, R.H., Mirkin, R.J., Tiddy, G.J.T., 1997. Langmuir 13 (14), 3706–3714.
Schoukens, G., De Clerck, K., 2005. Polymer 46, 845–857.
Silverstein, R.M., Basler, C.G., Morill, C.T., 1998. Spectrometric Identification of Organic Compounds. De Boeck.
Sutananta, W., Craig, D.Q.M., Newton, J.M., 1994. Int. J. Pharm. 111, 51–62.
Svensson, A., Neves, C., Cabane, B., 2004. Int. J. Pharm. 281 (1–2), 107–118.
Tardieu, Luzzati, 1970. Biochim. Biophys. Acta 219, 11–17.